

## Formation of uniform TiO<sub>2</sub> nanoshell on $\alpha$ -alumina nanoplates for effective metallic luster pigments

Su Jin Lee, Myoung Sang You, and Sang Hyuk Im<sup>†</sup>

Functional Crystallization Center (ERC), Department of Chemical Engineering, Kyung Hee University,  
1732 Deogyong-daero, Giheung-gu, Yongin-si, Gyeonggi-do 17104, Korea  
(Received 17 March 2016 • accepted 15 April 2016)

**Abstract**—To synthesize non-corroding effect pigment appearing metallic silver in color, we coated uniform anatase TiO<sub>2</sub> nanoshell via sol-gel chemistry. Under the reaction condition using 3 M TiCl<sub>4</sub> aqueous solution : deionized water : HCl solution=0.75 mL : 20 mL : 0 mL, ~50 nm-thick smooth TiO<sub>2</sub> nano-shell was fully coated on the surface of  $\alpha$ -alumina nanoplates; consequently, the synthesized effect pigments exhibited similar lustering effect and structuring color to commercial effect pigment. Under relatively acidic condition and higher TiCl<sub>4</sub> precursor concentration condition (3 M TiCl<sub>4</sub> aqueous solution : deionized water : HCl solution=0.75 mL : 20 mL : 0.05 mL for acidic condition and 1.0 or 1.5 mL : 20 mL : 0 mL for higher TiCl<sub>4</sub> precursor concentration condition), rougher TiO<sub>2</sub> shell was formed.

Keywords:  $\alpha$ -Alumina Nanoplates, TiO<sub>2</sub> Shell, Roughness Control, Effect Pigment, Metallic Silver Color

### INTRODUCTION

Silver is a shiny novel metal with face centered cubic (fcc) structure that gives a feeling of coolness, whereas gold gives us a warm feeling. So the metallic silver color has been used to express modern industrial design, riches, and classical design. The metallic silver color has been widely used in automobiles, jewelry, nail arts, notebook PCs, smart phone, and cosmetics [1-6].

Metallic silver absorbs light below ~380 nm-wavelength and reflects the whole visible wavelength region. Therefore, a CMYK (cyan-magenta-yellow-black) code of silver or silver white is (0%, 0%, 0%, <25%). Accordingly, one substrate should strongly reflect whole visible light to express metallic silver or silver white in color.

Although metallic silver has the highest reflectance in the visible region than other metals, it is likely to be tarnished by oxidation or reaction with other anions, so that an additional passivation layer is often required to prevent such color fading. The severe color tarnish of metallic silver might be associated with the fact that the color of silver oxide and silver sulfide is black or brown black, whereas the oxidized aluminum metal exhibiting metallic silver is transparent.

Industrially, it is important to mimic lustering metallic color by non-corrosive inorganic materials because they can maintain lustering color semi-permanently due to the inherently stable oxide form. A long time ago, these lustering effect pigments were obtained from the fish scales or hair tails of herring due to the lack of the synthetic technology for artificial lustering pigments. Guanine or hypoxanthine crystals can be used as natural lustering effect pigments, but their production yield and quality was not consistent. Therefore, synthetic lustering effect pigments such as basic lead carbonate, bismuth oxychloride, micaceous iron oxide, glass, and

$\alpha$ -alumina have been developed [1]. Among them, the crystalline  $\alpha$ -alumina nanoplates seem to be the best candidate for the lustering effect pigments due to uniform surface flatness, good hardness, high reflectivity, strong chemical resistivity, and chemical affinity to other metal oxides [1]. On the other hand, the other nanoplates, including natural and synthetic mica, cannot satisfy all industrial requirements.

Generally, the lustering effect and color of the effect pigments is controlled by the constructive and destructive interference between the nanoplate substrate and the coated shell on the nanoplate substrate. To maximize the lustering effect and control the color of the effect pigments, it is crucial to use a high refractive index material with finely controlled thickness for the shell material. Accordingly, here we chose the crystalline  $\alpha$ -alumina nanoplates and crystalline TiO<sub>2</sub> as substrate and shell material, respectively. Recently, we reported  $\alpha$ -alumina-TiO<sub>2</sub> core-shell nanoplates appearing metallic gold in color by coating relatively thick and rough TiO<sub>2</sub> shell on  $\alpha$ -alumina substrate, because the reflection color is dependent on the product of refractive index and thickness of TiO<sub>2</sub> shell [6]. As a rule of thumb, the thicker TiO<sub>2</sub> shell reflects the longer wavelength of light so that to reflect silver or silver white color the TiO<sub>2</sub> shell should be thin and have an even surface with small roughness. Therefore, the demonstration of lustering metallic silver in color from the inorganic effect pigments seems to be trickiest to demonstrate other colors. It is industrially important to demonstrate metallic silver in color by using non-corrosive inorganic materials which strongly reflect whole visible light similarly to metallic silver. Hence, we tried to demonstrate metallic silver color by coating very thin TiO<sub>2</sub> shell uniformly on the surface of  $\alpha$ -alumina nanoplates.

### EXPERIMENTAL

#### 1. Materials

Commercially available alumina nanoplates with TiO<sub>2</sub> shell

<sup>†</sup>To whom correspondence should be addressed.

E-mail: imromy@khu.ac.kr

Copyright by The Korean Institute of Chemical Engineers.

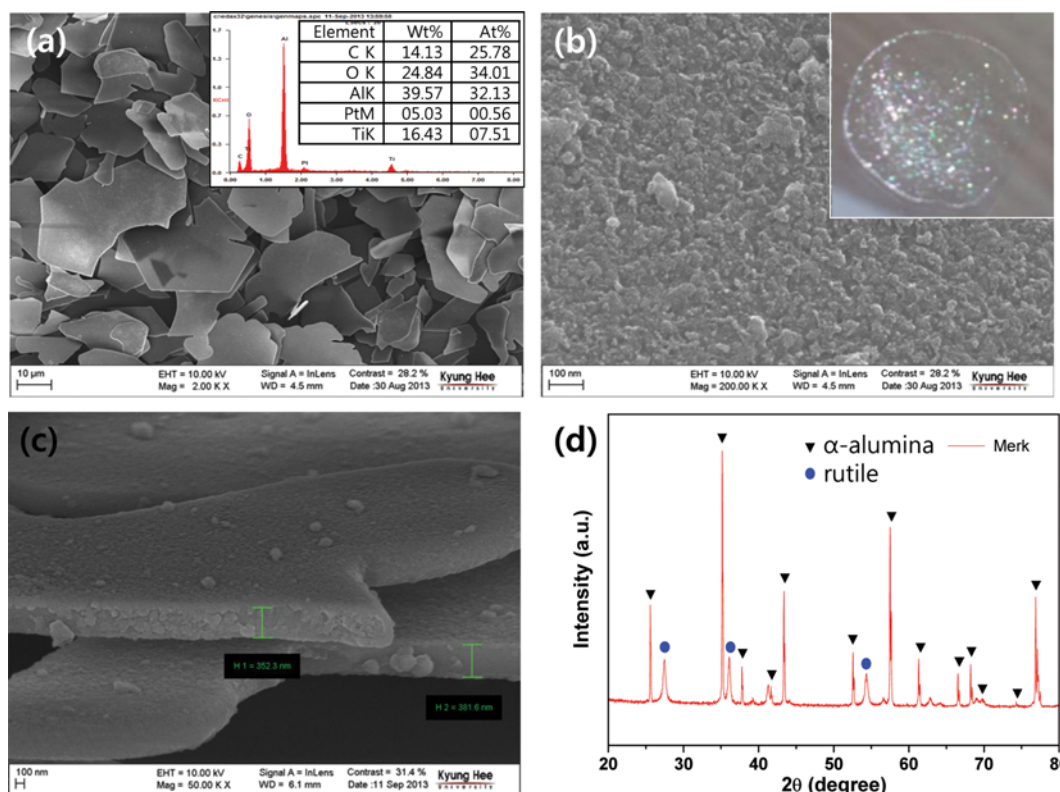


Fig. 1. (a) SEM image of commercially available alumina nanoplates with TiO<sub>2</sub> shell (Xirallic T60-10SW, Crystal silver, MERCK) lustering metallic silver white in color: the inset is EDS (energy dispersive X-ray spectroscopy) spectrum, (b) magnified SEM image of its surface: the inset is a photograph of dried alumina nanoplates with TiO<sub>2</sub> shell powder, (c) tilted SEM image showing cross-sectional morphology of alumina nanoplates with TiO<sub>2</sub> shell, and (d) XRD (X-ray diffraction) patterns of the sample.

(MERCK, Xirallic T60-10SW, Crystal silver) lustering metallic silver white in color,  $\alpha$ -alumina nanoplate (TCERA), TiCl<sub>4</sub> (Fluka), HCl (Samchun), and NaOH (Samchun) were used as received without further purification.

## 2. Characterization

The morphology of commercially available alumina nanoplates with TiO<sub>2</sub> shell (MERCK, Xirallic T60-10SW, Crystal silver) lustering metallic silver white in color,  $\alpha$ -alumina nanoplate (TCERA) and  $\alpha$ -alumina nanoplate with smooth TiO<sub>2</sub> shell was characterized by scanning electron microscopic (SEM: Supra 55, Carl Zeiss). For this, we dropped the nanoplates dispersion solution on a Si wafer and dried them in a convection oven at 60 °C for 30 min. Pt was then sputtered on the sample prior to examine the SEM image. The composition was analyzed by EDX (energy dispersive X-ray spectroscopy) equipped to SEM machine. For the analysis of transmission electron microscopic (TEM: Jem-2100F, Jeol) image of  $\alpha$ -alumina nanoplate with smooth TiO<sub>2</sub> shell, we dropped the nanoplate dispersion solution on a carbon coated Cu grid and subsequently dried it at 60 °C for 30 min. Its composition was analyzed by EDX (energy dispersive X-ray spectroscopy) equipped to TEM machine. Their crystal structures were characterized by X-ray diffraction (XRD: D8 Advance, Bruker) machine. For this, we dropped the nanoplate dispersion solution on a Si low background sample holder and subsequently dried it. We scanned the samples from 20° to 80° at a scan rate of 6°/min under irradiation of Cu K- $\alpha$  ( $\lambda=0.15406$  nm).

## RESULTS AND DISCUSSION

Fig. 1 is the morphology and structure characterization of commercially available alumina nanoplates with TiO<sub>2</sub> shell (Xirallic T60-10SW, Crystal silver, MERCK) lustering metallic silver white. The SEM (scanning electron microscopic) surface image of them indi-

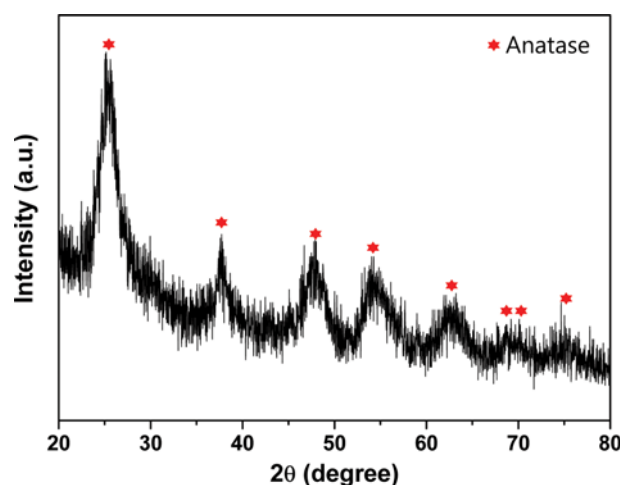


Fig. 2. XRD pattern confirming that the produced TiO<sub>2</sub> nanoparticles are anatase phase.

cates that the lateral size of alumina nanoplates with TiO<sub>2</sub> shell is 10–40 μm (Fig. 1(a)). The inset is EDS spectrum of alumina nanoplates with TiO<sub>2</sub> shell, indicating that it is composed of alumina and TiO<sub>2</sub>, of which the atomic ratio of Al to Ti is 32.1 to 7.5. The magnified SEM image of its surface (Fig. 1(b)) clearly shows that its surface is fully covered by relatively smooth TiO<sub>2</sub> nanoparticles. The inset is a photograph of dried powder of commercially available alumina nanoplates with TiO<sub>2</sub> shell, indicating that they exhibit metallic silver white and some particles show greenish structuring color like one-dimensional photonic crystal. This implies that the thickness of TiO<sub>2</sub> shell is very uniform. The tilted SEM image in Fig. 1(c) shows the cross-sectional morphology alumina nanoplates with TiO<sub>2</sub> shell, indicating that its thickness is 350–400 nm and the thickness of the TiO<sub>2</sub> shell is <50 nm. Fig. 1(d) is XRD (X-ray diffraction) patterns

of alumina nanoplates with TiO<sub>2</sub> shell, indicating that it is composed of crystalline  $\alpha$ -alumina as a substrate and crystalline rutile TiO<sub>2</sub> as a shell material.

Generally, crystalline rutile and anatase TiO<sub>2</sub> phase can be formed by sol-gel solution process. TiCl<sub>4</sub> precursor is widely adapted to synthesize TiO<sub>2</sub> nanocrystals because TiCl<sub>4</sub> can make stable TiOCl<sub>2</sub> intermediate phase in water, and consequently it is an environmentally friendly process compared to alkoxide based titanium precursor. Here, we used 3 M TiCl<sub>4</sub> aqueous solution, of which stable TiOCl<sub>2</sub> intermediate phase is formable and the solution is very stable. When we dilute the 3 M TiCl<sub>4</sub> solution with deionized water, the pH of the solution is increased and sol-gel reaction is thus promoted by hydrolysis and condensation reaction mechanism. The reactant solution forms  $[\text{Ti}(\text{OH})_m\text{Cl}_n]^{2-}$  ( $m+n=6$ ) octahedral intermediate units,

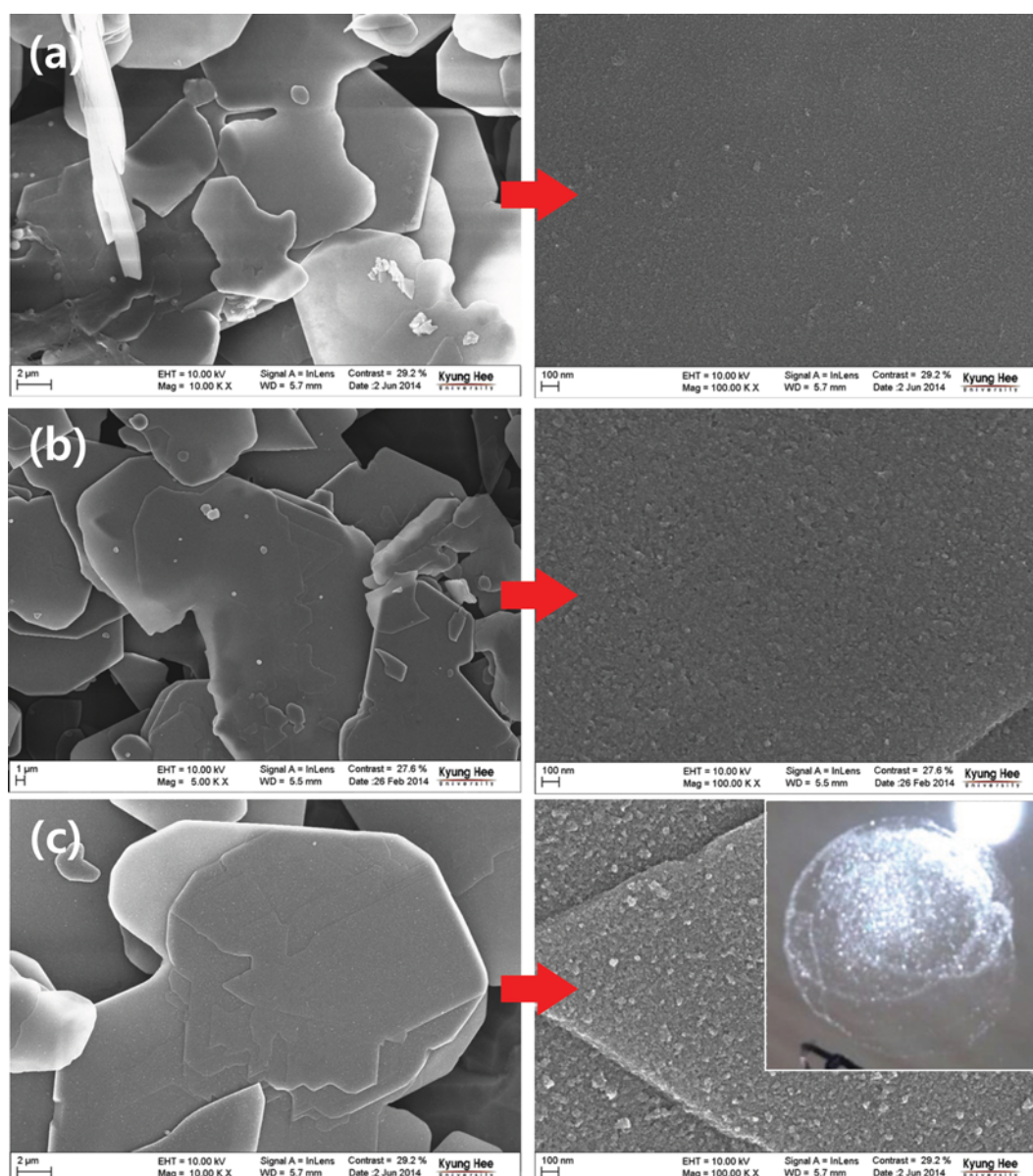


Fig. 3. SEM images of  $\alpha$ -alumina nanoplates coated by TiO<sub>2</sub> shell with reaction time (a) 1 h, (b) 3 h, and (c) 5 h: inset=photograph of dried powder of  $\alpha$ -alumina nanoplate by TiO<sub>2</sub> shell. Right SEM images are magnified images of the surface of TiO<sub>2</sub> shell on  $\alpha$ -alumina nanoplate (reaction condition=3 M TiCl<sub>4</sub> aqueous solution : deionized water : HCl solution=0.75 mL : 20 mL : 0.05 mL).

and the ratio of  $m$  to  $n$  is dependent on the pH and presence of Cl<sup>-</sup> [7]. In more acidic condition under presence of Cl<sup>-</sup>,  $n$  is dominated so that the octahedral units tend to be bridged together through corner sharing, thereby producing rutile crystalline phase. Meanwhile, in less acidic condition,  $m$  is dominated and multiple hydroxyl groups in octahedral unit tend to be bridged together via edge sharing, thereby producing anatase crystalline phase. Typically, the rutile crystals form needle-shaped crystals so that one-dimensional morphology such as rod and wire is easily grown on a crystalline substrate with small lattice parameter mismatch from rutile crystal. The anatase crystals tend to form relatively spherical shape so that this has the benefit to form a smoother surface than rutile phase. The lustering effect is dependent on the refractive index and roughness of TiO<sub>2</sub> shell because the reflectance is increased as

the difference of refractive index between two adhering materials ( $\alpha$ -alumina and TiO<sub>2</sub>) becomes larger, and more distinctive color can be expressed by the smoother surface of TiO<sub>2</sub> shell due to reduced random back scattering. Here, we focus on the formation of smoother anatase TiO<sub>2</sub> shell to make a difference from the commercially available alumina plates with rutile TiO<sub>2</sub> shell (Xirallic T60-10SW, MERCK).

In our previous report, we found that the pure anatase phase TiO<sub>2</sub> is formed at the reaction condition of 3 M TiCl<sub>4</sub> aqueous solution : deionized water : HCl solution = 0.5 mL : 20 mL : 0-0.1 mL [6]. In a typical process for the formation of anatase TiO<sub>2</sub> shell on the surface of  $\alpha$ -alumina nanoplate (TCERA), we first added 0.05 g  $\alpha$ -alumina nanoplates in 20 mL deionized water charged in a vial. And HCl solution (0 mL or 0.05 mL) was added in the deionized water. The reactant solution was then mixed by magnetic stirrer and was

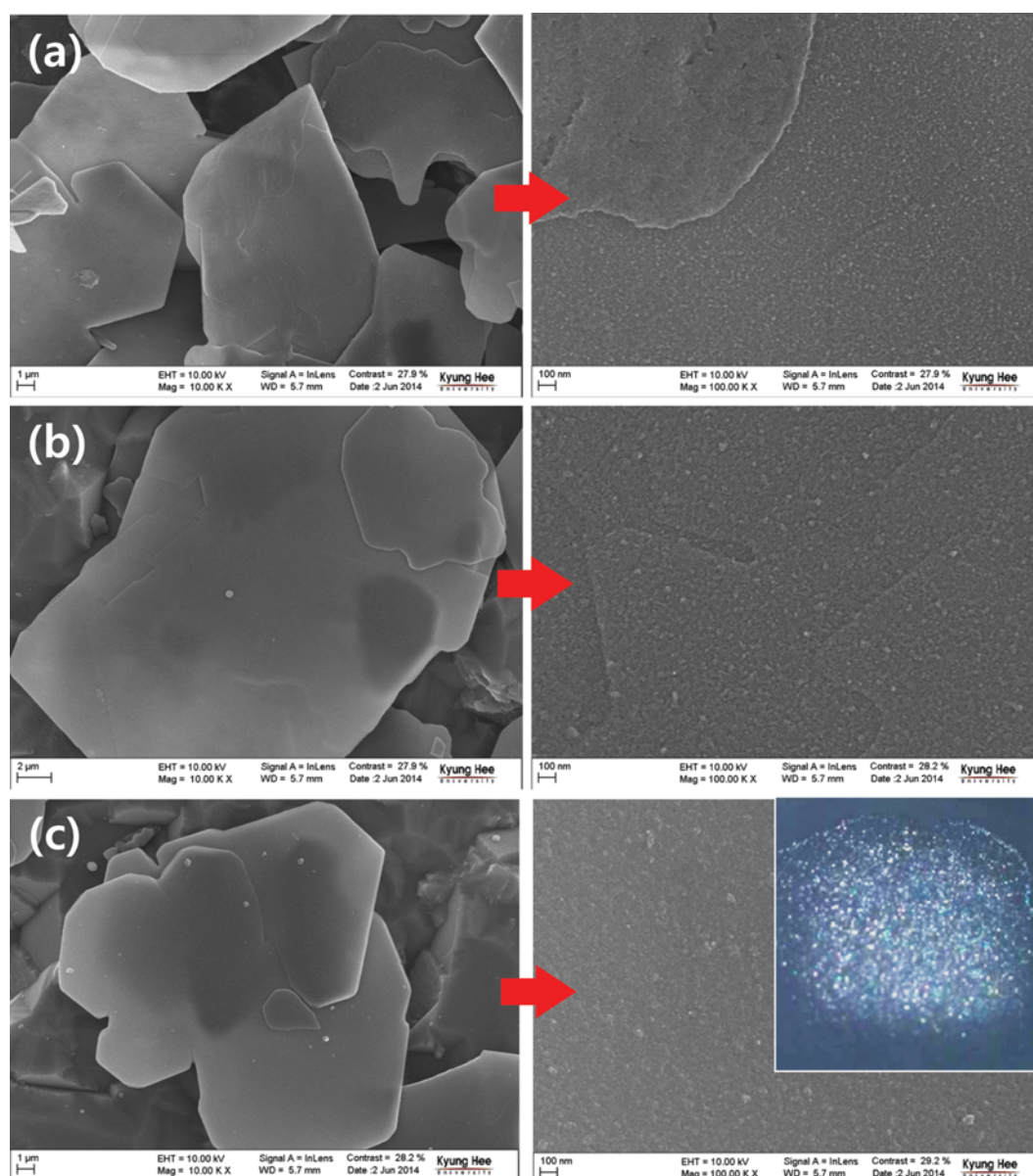


Fig. 4. SEM images of  $\alpha$ -alumina nanoplates coated by TiO<sub>2</sub> shell with reaction time (a) 1 h, (b) 3 h, and (c) 5 h: inset=photograph of dried powder of  $\alpha$ -alumina nanoplate by TiO<sub>2</sub> shell. Right SEM images are magnified images of the surface of TiO<sub>2</sub> shell on  $\alpha$ -alumina nanoplate (reaction condition = 3 M TiCl<sub>4</sub> aqueous solution : deionized water : HCl solution = 0.75 mL : 20 mL : 0 mL).

heated to 98 °C. Then 0.75 mL 3 M  $\text{TiCl}_4$  precursor aqueous solution was added in the solution drop by drop. The reaction was proceeded for 5 h. When we added 0.5 mL 3 M  $\text{TiCl}_4$  precursor aqueous solution above experimental condition, the coverage of  $\text{TiO}_2$  shell was not perfect so here we added 0.75 mL  $\text{TiCl}_4$  precursor aqueous solution to ensure full surface coverage of  $\text{TiO}_2$  shell on the  $\alpha$ -alumina nanoplate. When we checked the XRD pattern of produced nanoparticles after sol-gel reaction of the above solutions without  $\alpha$ -alumina nanoplates for 1 h, the pure anatase crystalline  $\text{TiO}_2$  was formed similarly to the results of previous report (Fig. 2).

To check the morphological evolution of  $\text{TiO}_2$  shell in the sample (3 M  $\text{TiCl}_4$  aqueous solution : deionized water : HCl solution = 0.75 mL : 20 mL : 0.05 mL) with reaction time, we chose the sam-

ple with reaction time ( $t=1$  h, 3 h, and 5 h) and examined SEM morphology images as shown in Fig. 3. The SEM images indicate that the surface  $\alpha$ -alumina nanoplate (TCERA) was fully covered by  $\text{TiO}_2$  nanoparticles and the surface of  $\text{TiO}_2$  shell was gradually rougher with reaction time due to the continuous over growth of  $\text{TiO}_2$ . An inset is a photograph of the dried  $\alpha$ -alumina nanoplate with  $\text{TiO}_2$  shell powder on a glass substrate, indicating that the produced powder shows silver white color, but lustering intensity was slightly weaker compared to commercially available alumina plates with rutile  $\text{TiO}_2$  (Xirallic T60-10SW, MERCK). In addition, we could not see strong structuring color effect by constructive and destructive interference even though the sample exhibited slight greenish color.

To reduce the over-growth of  $\text{TiO}_2$  shell and to ensure the for-

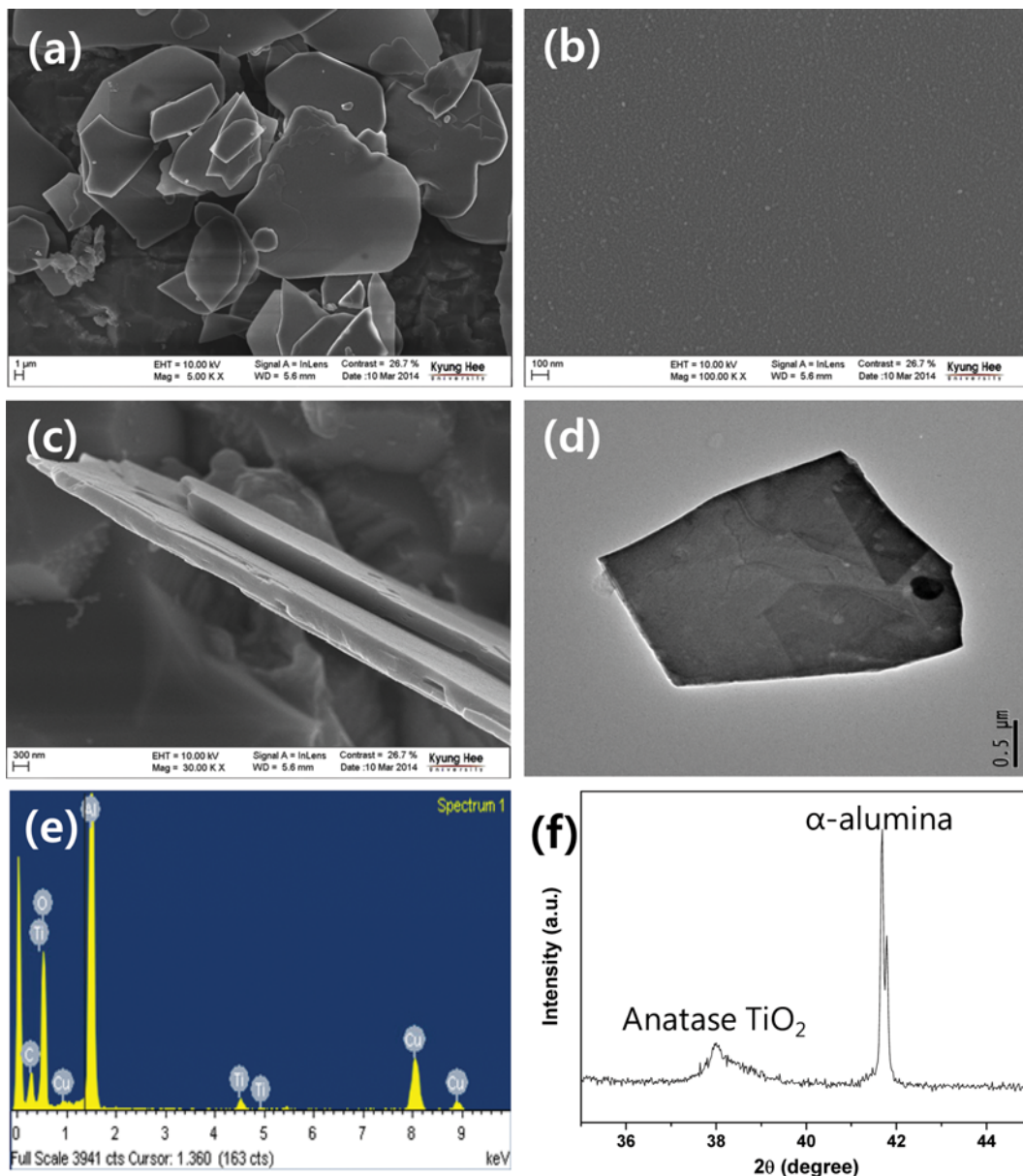


Fig. 5. The morphology and structure characterization of the heat-treated  $\alpha$ -alumina nanoplates with smooth  $\text{TiO}_2$  shell at 500 °C (reaction condition = 3 M  $\text{TiCl}_4$  aqueous solution : deionized water : HCl solution = 0.75 mL : 20 mL : 0 mL). (a), (b), (c) SEM surface and tilted images, (d) TEM image, (e) EDX spectrum, and (f) XRD pattern.

mation of smoother TiO<sub>2</sub> shell, we reduced the concentration of acid catalyst by removing the added HCl solution. The SEM morphology evolution of TiO<sub>2</sub> shell in the sample (3 M TiCl<sub>4</sub> aqueous solution : deionized water : HCl solution = 0.75 mL : 20 mL : 0 mL) with reaction time is shown in Fig. 4. The SEM images clearly confirm that the surface of all  $\alpha$ -alumina nanoplates was fully covered by small TiO<sub>2</sub> nanoparticles irrespective of the reaction time. Apparently, the formed TiO<sub>2</sub> shell has smaller roughness and is denser than the sample in Fig. 3. The inset photograph in Fig. 4 indicates that the produced  $\alpha$ -alumina nanoplates with TiO<sub>2</sub> shell show silver white color and strong lustering effect similar to commercially available sample (Xirallic T60-10SW, MERCK). In addition, the produced sample also exhibits structuring color effect because greenish reflecting color also appears. The apparent feature including color and glittering was almost same as the commercially available sample. Note that the  $\alpha$ -alumina nanoplates with smoother anatase TiO<sub>2</sub> shell than the commercial  $\alpha$ -alumina nanoplates with rutile TiO<sub>2</sub> shell can exhibit similar feature to the commercial one. When we increased the amount of 3 M TiCl<sub>4</sub> precursor aqueous solution from 0.75 mL to 1.0 mL and 1.5 mL, the surface of TiO<sub>2</sub> shell was more roughened as shown in Fig. S1 due to more over-growth of TiO<sub>2</sub>.

Finally, we heat-treated the  $\alpha$ -alumina nanoplates with smooth TiO<sub>2</sub> shell (Fig. 4 sample) at 500 °C to improve the adhesiveness between TiO<sub>2</sub> shell and  $\alpha$ -alumina nanoplate. Fig. 5(a) and (b) is the SEM image of  $\alpha$ -alumina nanoplates with smooth TiO<sub>2</sub> shell with heat-treatment at 500 °C, indicating that the topology and roughness is maintained by heat-treatment. Fig 5(c) is a tilted SEM image for cross-sectional morphology of  $\alpha$ -alumina nanoplate with smooth TiO<sub>2</sub> shell with heat-treatment at 500 °C, indicating that the thickness of the plates is ~500 nm and the thickness of TiO<sub>2</sub> shell is ~50 nm. The TEM (transmission electron microscopy) image in Fig. 5(d) exhibited even contrast, implying the formation of uniform TiO<sub>2</sub> shell. The EDX spectrum in Fig. 5(e) and the XRD pattern in Fig. 5(f) confirm that anatase TiO<sub>2</sub> shell is formed on the surface of  $\alpha$ -alumina nanoplates.

## CONCLUSIONS

We could synthesize  $\alpha$ -alumina nanoplates with smooth anatase TiO<sub>2</sub> shell appearing metallic silver in color, of which feature is almost the same as commercially available  $\alpha$ -alumina nanoplates with rutile TiO<sub>2</sub> shell (Xirallic T60-10SW, MERCK). To form anatase phase TiO<sub>2</sub> shell, we coated the TiO<sub>2</sub> shell through the reaction condition of 3 M TiCl<sub>4</sub> aqueous solution : deionized water : HCl solution = 0.75 mL : 20 mL : 0.1 or 0 mL. Under relatively acidic condition (3 M TiCl<sub>4</sub> aqueous solution : deionized water : HCl solution =

0.75 mL : 20 mL : 0.05 mL), the roughness of TiO<sub>2</sub> shell was gradually rough with reaction time so that the lustering effect was poorer than the conventional  $\alpha$ -alumina nanoplates with rutile TiO<sub>2</sub> shell. However, under the reaction condition of 3 M TiCl<sub>4</sub> aqueous solution : deionized water : HCl solution = 0.75 mL : 20 mL : 0 mL very smooth TiO<sub>2</sub> shell was coated on the  $\alpha$ -alumina nanoplates irrespective of the reaction time and exhibited similar lustering effect and structuring color to the commercially available one. The heat-treated  $\alpha$ -alumina nanoplates with smooth anatase TiO<sub>2</sub> shell at 500 °C were conducted to ensure the adhesion between  $\alpha$ -alumina nanoplate and TiO<sub>2</sub> shell, and the heat-treated samples had similar features as the sample without heat-treatment. We believe that the synthesized  $\alpha$ -alumina nanoplates with smooth anatase TiO<sub>2</sub> shell appearing metallic silver in color can be used as effective pigments for automobiles and cosmetics or effective light back scattering filler for solar cells [8,9].

## ACKNOWLEDGEMENTS

S. J. Lee and M. S. You contributed equally to this study. This study was supported by Basic Science Research Program (No. 2014R1A5A1009799) through the National Research Foundation of Korea (NRF) funded by the Ministry of Science, ICT & Future Planning.

## SUPPORTING INFORMATION

Additional information as noted in the text. This information is available via the Internet at <http://www.springer.com/chemistry/journal/11814>.

## REFERENCES

1. M. Debeljak, A. Hladnik, L. Cerne and D. Gregor-Svetec, *Color Res. Appl.*, **38**, 168 (2012).
2. G. Pfaff, *Inorg. Mater.*, **39**, 123 (2003).
3. V. Štengl, J. Šubrt, S. Bakardjieva, A. Kalendova and P. Kalenda, *Dyes Pigm.*, **58**, 239 (2003).
4. S. Teaney, G. Pfaff and K. Nitta, *Eur. Coat. J.*, **4**, 90 (1999).
5. S. Sharrock and N. Schuel, *Eur. Coat. J.*, **1/2**, 20 (2000).
6. M. W. Suh, S. J. Lee, M. S. You, S. B. Park and S. H. Im, *RSC Adv.*, **5**, 56954 (2015).
7. H. Cheng, J. Ma, Z. Zhao and L. Qi, *Chem. Mater.*, **7**, 663 (1995).
8. J. Yang, Y. Lin and Y. Meng, *Korean J. Chem. Eng.*, **30**, 2026 (2013).
9. V. B. Chu, S. J. Park, G. S. Park, H. S. Jeon, Y. J. Hwang and B. K. Min, *Korean J. Chem. Eng.*, **33**, 880 (2016).

## Supporting Information

### Formation of uniform $\text{TiO}_2$ nanoshell on $\alpha$ -alumina nanoplates for effective metallic luster pigments

Su Jin Lee, Myoung Sang You, and Sang Hyuk Im<sup>†</sup>

Functional Crystallization Center (ERC), Department of Chemical Engineering, Kyung Hee University,  
1732 Deogyong-daero, Giheung-gu, Yongin-si, Gyeonggi-do 17104, Korea

(Received 17 March 2016 • accepted 15 April 2016)

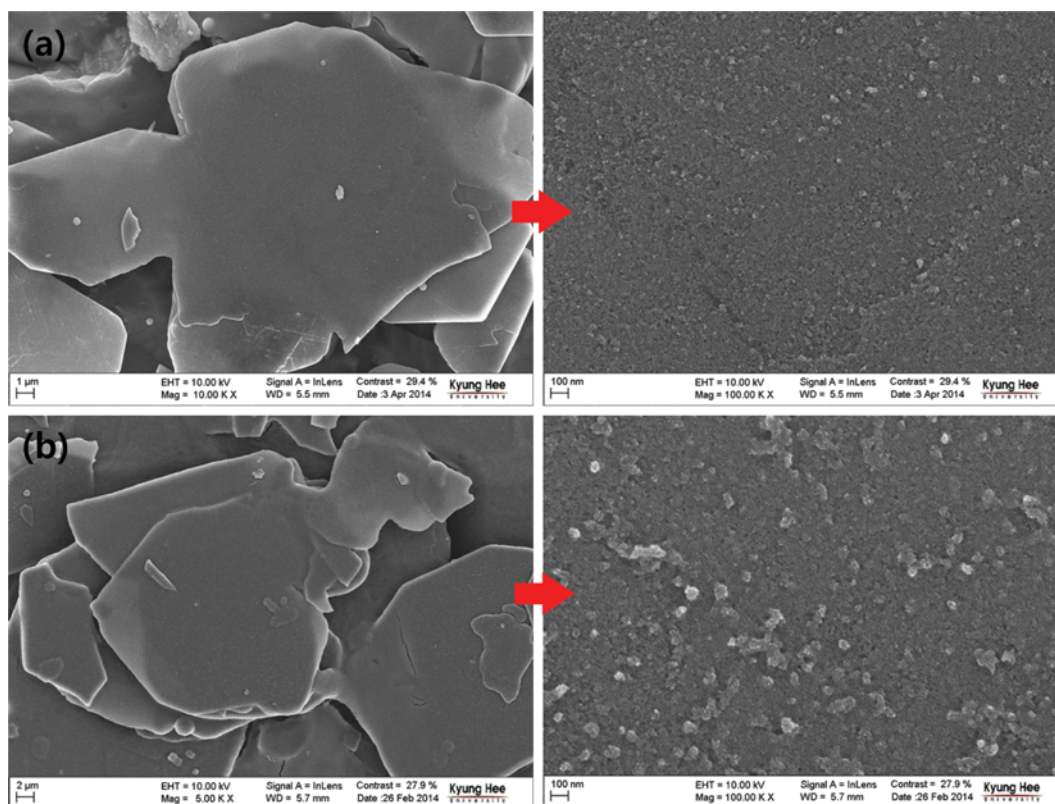


Fig. S1. The SEM images of  $\alpha$ -alumina nanoplates coated by  $\text{TiO}_2$  shell formed under increased amount of 3 M  $\text{TiCl}_4$  precursor aqueous solution to (a) 1.0 mL and (b) 1.5 mL (reaction condition=3 M  $\text{TiCl}_4$  aqueous solution : deionized water : HCl solution=1.0 or 1.5 mL : 20 mL : 0 mL).